Available online at www.sciencedirect.com
ScienceDirect
Microelectronic Engineering 84 (2007) 2450–2454
MICROELECTRONIC ENGINEERING
www.elsevier.com/locate/mee

CoWBP capping barrier layer for sub 90 nm Cu interconnects

R. Ofek Almog [a,*], Y. Sverdlov [a], I. Goldfarb [b], Y. Shacham-Diamand [a]

[a] Department of Physical Electronics, Tel-Aviv University, Tel-Aviv 69978, Israel
[b] Department of Solid Mechanics, Materials and Structures, Tel-Aviv University, Tel-Aviv 69978, Israel

Received 15 May 2007; accepted 21 May 2007
Available online 26 May 2007

Abstract

Electroless cobalt films have been obtained by deposition using a plating bath containing two reducing agents: dimethylamineborane (DMAB) and sodium hypophosphite. This formulation allows spontaneous activation on copper followed by auto catalytic electroless plating. CoWBP and CoBP films are proposed as diffusion barriers and encapsulation layers, for copper lines and via contacts for ULSI interconnect applications. The crystalline structure, chemical composition and oxidation states of the elements were studied, as well as the electrical resistivity, topography and morphology of the films. The film composition was characterized as a function of the solution composition; the barrier properties of the films were tested and an oxidation resistance study was conducted. The films were characterized and the results show that they can be applied as capping layers for ULSI copper metallization.

Keywords: Cobalt; Tungsten; Phosphorous; Boron; Electroless deposition

1. Introduction

ULSI interconnects are made of copper due to its high resistance to electromigration and stress voiding and its low resistivity. However, there are a few major problems with copper metallization. Copper diffusion through the adjacent insulators into the semiconductor results in device or inter-level dielectric failure. Additionally, copper oxidation must be prevented during the steps coming after chemical–mechanical polishing (CMP) planarization [1,2] and cleaning steps that are essential to the damascene process.

Electroless deposition has been recently introduced in micro and nano technologies for depositing barriers against Cu diffusion in advanced microelectronic devices due to its low processing temperature and selectivity [3].

Recent application of ternary cobalt based layers as diffusion barriers and capping layers for Cu metallization improves interconnection performance and solves some critical problems such as maintaining low interconnect resistance while preventing contamination by copper [4,5] and improving the electromigration lifetime [6]. Adding phosphorous or boron enables deposition of amorphous or nano-crystalline films with relatively low grain boundary Cu diffusivity. Adding tungsten, or other refractory metals, may further improve the thin film barrier properties by forming either ''stuffed'' polycrystalline or amorphous diffusion barrier. In some cases electroless cobalt alloys from an amorphous phase with an embedded nano-crystalline structure [7,8].

The advantages of electroless CoWP alloys were shown by Shacham-Diamand et al. [8,9] and its deposition mechanisms and properties were discussed. One major problem in cobalt phosphorous alloy deposition is that Pd seeding was necessary to start the electroless plating reaction at the Cu surfaces. It was shown that employment of an electroless plating bath with boron containing reducing agent can initiate thin film electroless plating [10]. ''Pd free'' processes may also require a preliminary surface treatment of the Cu surface prior to the cobalt electroless plating [10]. The advantages of combining two reducing agents in the electroless plating bath: hypophosphite as a source for phosphorus and dimethylamineborane as a source for boron, are: (a) Pd-free deposition and (b) adding another

* Corresponding author. Tel.: +972 3 6406284; fax: +972 3 642 3508.
E-mail address: ofek.almog@gmail.com (R.O. Almog).

0167-9317/$ - see front matter © 2007 Elsevier B.V. All rights reserved.
doi:10.1016/j.mee.2007.05.031

parameter for the thin film properties control. Similar to the previously discussed CoWP [5,6] and CoWB [10], CoWBP alloys also demonstrated high stability under thermal treatment in vacuum.

2. Experimental

Sputtered Cu seed (~5 nm) on SiO_2/Si system was used as a substrate. A 15 nm thick titanium film was sputtered on the silicon oxide prior to the Cu seed in order to improve adhesion between the Cu layer and the oxide. Electroless deposition was carried out without Pd-activation. The treatment of the surface in 2–10% DMAB solution serves as an activating step.

Electroless deposition of CoWBP and CoBP was performed on the copper surface from sulfate-citrate electroless baths with dimethylamineborane (DMAB) as the primary reducing agent and source for boron. Sodium hypophosphite was used as second reducing agent and a source for phosphorous. Tri-sodium citrate was used as a complexing agent to form strong cobalt complexes. The working pH value of 9.5–9.7 was maintained by potassium hydroxide. The concentration of NaH_2PO_2 was either 1 or 7.3 g/l in order to study its effect on the thin film composition and properties. Sodium tungstate (Na_2WO_4) was employed as a source for tungsten for CoWBP (Table 1). The tungstate concentration in the CoWBP deposition bath was kept constant at 1 g/l (0.003 M). All chemicals were analytical purity grade.

Electroless deposition was performed at 80–85 °C in a temperature controlled cell. The CoWBP and CoBP layers thickness was controlled by deposition time and were in the range of 6–97 nm. Post-deposition vacuum annealing was performed in vacuum under residual pressure less than 2×10^{-7} Torr at 350 °C, 450 °C and 550 °C for 1 h.

The thin film thickness, composition, and electrical properties were characterized. The layer thickness was measured using Tencor "Alpha-step 500" profilometer. Thin films composition after deposition and after annealing, and oxidation states were measured using XPS (X-ray photoelectron spectroscopy) 5600 Multi Technique PHI.

The sheet resistance and resistivity of the films were measured by the in-line four point probe made by Lucas/Signatone™. TEM images and electron diffraction were carried out using a high resolution TEM model Philips Tecnai F20 and HRSEM images were taken by a cold field emitter high resolution SEM model JEOL 6700F.

3. Results and discussion

Electroless deposited CoWBP and CoBP thin films demonstrated high adhesion to the substrate, uniformity over the sample surface and good coverage. The deposition reaction has an autocatalytic nature and the layer thickness is controlled by deposition time and reagent concentration in solution.

3.1. Deposition rate

The deposition rate was ~40 nm/min for the solution with DMAB only and it dropped to ~16 nm/min when the hypophosphite ion was added (Fig. 1). The deposition rate of CoBP is ~10 nm/min, which is slightly lower than that of CoWBP.

3.2. Copper diffusion into CoBP and CoWBP

The barrier properties of the films were tested by XPS profiling after annealing in vacuum at 350 °C, 450 °C and 550 °C for 1 h. For CoBP films with the thicknesses of 128.5 Å and 55.7 Å, a significant amount of copper diffusion occurred into the film after annealing at 450 °C. In CoBP films with a thickness of 321.2 Å, only minor amount of diffusion occurred at this temperature. However, in CoWBP films that were deposited from solutions with $[P] = 1$ g/l and with $[P] = 7.3$ g/l, there was no significant diffusion at this temperature. Copper diffusion into the CoWBP thin film could be seen after annealing at 550 °C. (Fig. 2).

Table 1
Solution composition for electroless deposition of CoWBP and CoBP films

	Material		Mw [g]	Concentration g/l (Molar)
	Name	Formula		
Role				
Co source	Cobalt sulphate heptahydrate	$CoSO_4 \cdot 7H_2O$	281	0.1 (28.1)
	DMAB	$(CH_3)_2NHBH_3$	58	0.069 (4)
Reducing agent	Sodium hypophosphite	NaH_2PO_2	111	0.0094 (1) or 0.069 (7.3)
W source	Sodium tungstate	Na_2WO_4	330	0 (0) or 0.003 (1)
Complexing agent	Sodium citrate	$Na_3C_6H_5O_7 \cdot 2H_2O$	294.1	0.3
Additive	Hydrogen chloride	HCl	36.5	(0.083)
Additive	Surfactant RE-610			1.5×10^{-2} cc/l
Variable				Value
pH		Adjusted by adding NaOH		9.5–9.7
Temp. [°C]				80–85

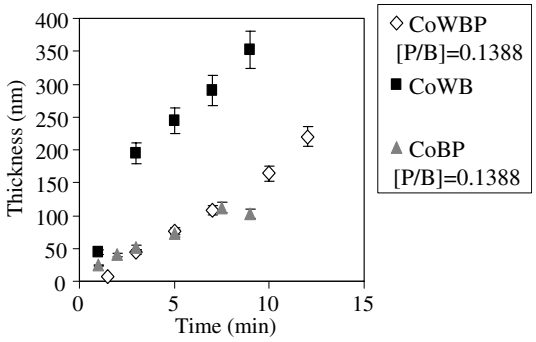

Fig. 1. Thickness of electroless CoWBP films as a function of deposition time.

3.3. Resistivity

The sheet resistance was measured after deposition and after thermal treatments at 350 °C, 450 °C, 550 °C and 650 °C for 1 h, in vacuum. The sheet resistance of CoWBP films is in the range of 2.3 Ω/sq. After thermal treatment at 350 °C the sheet resistance decreased to 1.8 Ω/sq. Further treatment at at 450 °C did not change the sheet resistance while the sheet resistance increased after thermal treatment at 550 °C and 650 °C to 2.7 Ω/sq and 2.8 Ω/sq, respectively. The decrease at 350 °C is due to the annealing of the film, and the increase at 550 °C and 650 °C is due to interdiffusion between the Co and the Cu, creating a Co–Cu alloy. The resistivity of CoWBP films is in the range of 20–32 μΩ cm $\pm\Delta R$ where $\Delta R/R$ was estimated to be in the range of 10–20%. The resistivity value was extracted by taking into consideration the thin copper film on which the CoWBP films were deposited; the measurement includes the parallel resistance of the copper field, therefore since both the Cu and the CoWBP are thin there is a significant error in the range of ±20% for CoWBP films thinner than 300 Å.

Even when assuming the worst case value for the resistivity it can be concluded that the sheet resistance and the resistivity of CoWBP is low in comparison to other common barrier layers such as TaN or WN.

3.4. Structure characterization

Electron diffraction showed a pattern of concentric sharp circles of high intensity (Fig. 3). They were identified as diffraction patterns from copper and α cobalt planes, as follows: diffractions from the hexagonal cobalt phase were from (100) plane, $d = 2.165$Å and from (102) plane, $d = 1.48$ Å. Diffractions from copper phase from the (111), (200), (220), (222) and (311) planes. One diffraction at $d = 2.44$ Å might be from CoB (101) plane.

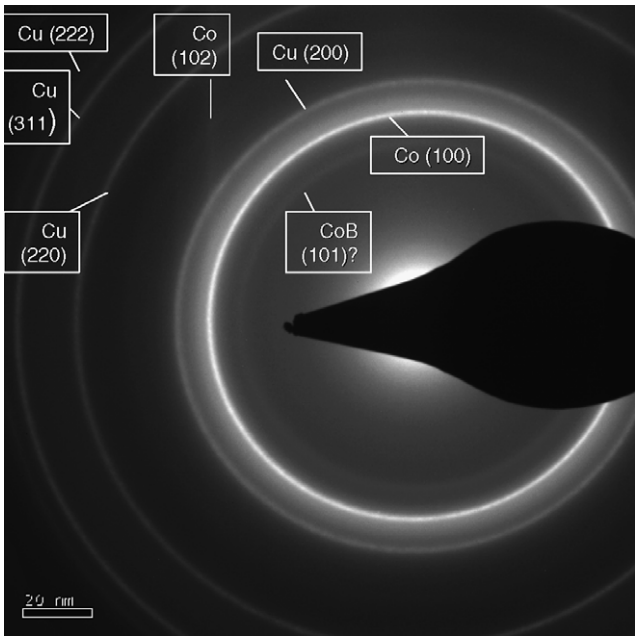

Fig. 3. Electron diffraction of CoBP (made from solution where $[H_2PO_2^-] = 1g/l$, see Table 1).

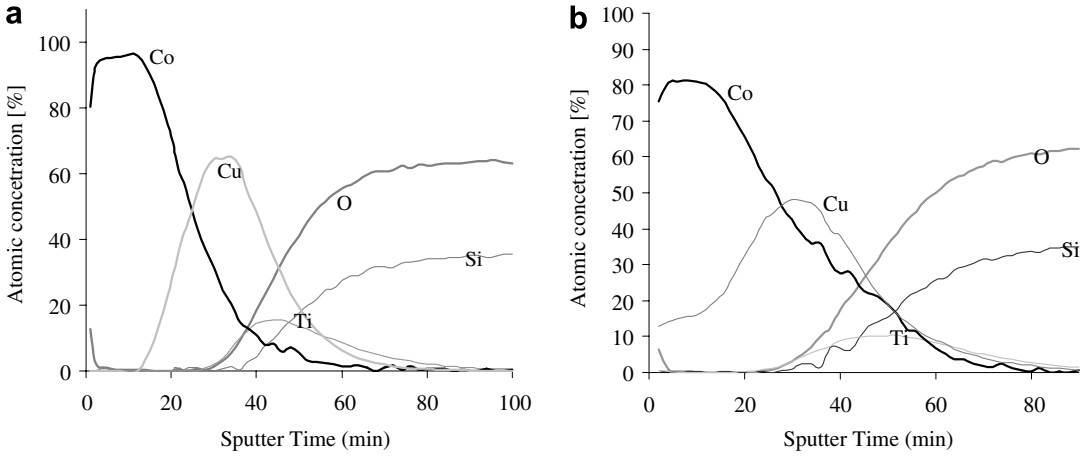

Fig. 2. Copper diffusion into CoWBP, $[H_2PO_2^-]/[DMAB] = 1$, XPS profile (a) as deposited and (b) after annealing at 550 °C for 1 h.

The concentric sharp circles indicate a randomly oriented poly crystals, and the diffractions from the cobalt phase indicates a hexagonal microstructure.

3.5. Morphology

In order to determine the crystalline structure of the films, high resolution TEM analysis was performed. The structure of the films after deposition was mostly amorphous with an embedded nano-crystalline structure. The size of most of the crystallites is in the range of 4–7 nm. However, there are some larger grains with dimension in the range of 10–12 nm (Fig. 4).

3.6. Concentration model

Electroless deposition of CoWPB alloy thin layers was performed on copper surface from sulfate-citrate electroless bath with DMAB and sodium hypophosphite as reducing agents. Concentration of NaH_2PO_2 was varied in range of 0–8.05 g/l in order to study its effect on the thin film content and properties. The sodium tungstate was employed as a source for tungsten. Its concentration was constant at 1 g/l (0.003 M). The film composition was characterized as a function of the solution composition using XPS and SIMS analysis. The results indicated that the film's composition is most likely determined by the reducing agents' co-adsorption rates.

A complete adsorption limited deposition model that formulates the dependence between the concentration of the reducing agents and the concentration of the cobalt, boron and phosphorous in the solid film was presented elsewhere [11]. A complete model was devised and compared successfully to the results.

For example, the dependence of the boron concentration in the film on the ratio of the two reducing agents is given by

$$\frac{[B]_{\mathrm{Film},0}}{[B]_{\mathrm{Film}}} = 1 + k_{\mathrm{B}}1.\frac{[\mathrm{H_2PO_2^-}]}{[\mathrm{DMAB}]} \quad (1)$$

Where $[B]_{\mathrm{Film}}$ is the concentration of boron in the film, $[B]_{\mathrm{Film},0}$ is the concentration of boron in the film at the beginning, k_{Bl} is a constant (as explained elsewhere [11]), $[\mathrm{H_2PO_2^-}]$ and [DMAB] are the hypophosphite and DMAB concentrations, respectively.

The results of the boron concentration are plotted in Fig. 5 as the inverse of the boron concentration vs. the hypophosphite to DMAB concentration ratio. It shows a linear relation over the entire range starting where the phosphorous concentration equals zero. This is due to the competition between the hypophosphite and DMAB during their initial surface adsorption that is prior to the actual co reduction. Therefore as the hypophosphite concentration in the solution increases, less DMAB is adsorbed. As a result, the boron concentration in the film decreases as the concentration of the phosphorous ions in the solution increases. The theoretical results seem to yield a similar function to that of what we found experimentally.

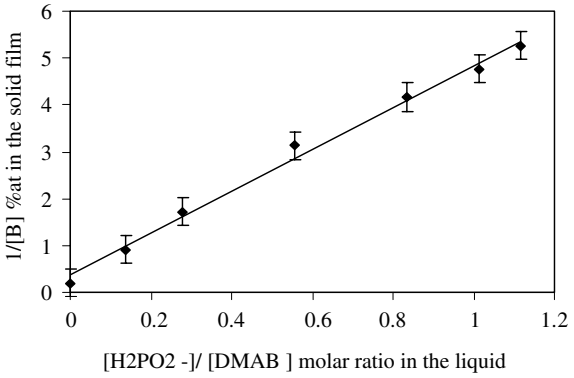

Fig. 5. Boron concentration as a function of the concentration of the reducing agents in a CoWBP film.

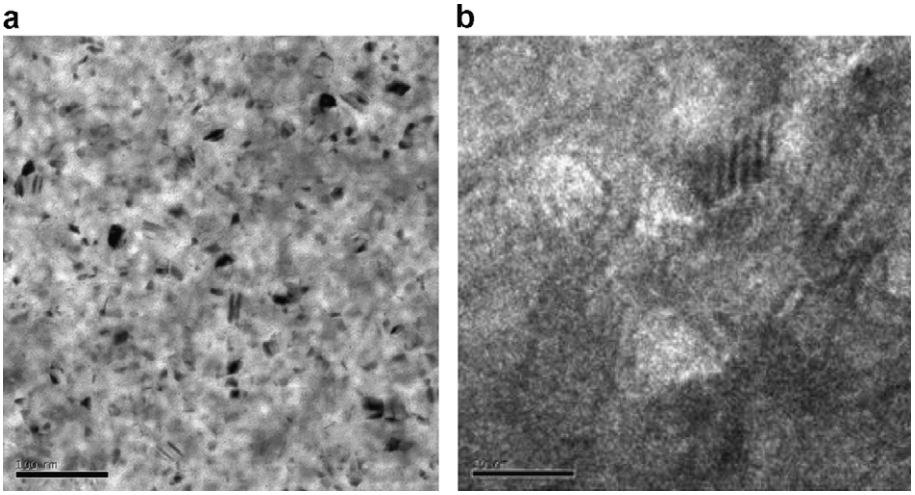

Fig. 4. Bright field TEM plan view images of CoBP films, as-deposited, (a) ×38 K and (b) ×400 K.

4. Conclusions

The electroless deposition of cobalt alloys system with two reducing agents was studied. Using both sodium hypophosphite and DMAB reducing agents with cobalt metal ionic solution and tungstate ions at a lightly basic solution results in a self activated spontaneous deposition of CoWPB thin-film coatings formation.

The solution composition was studied; the functional dependence between the solid to the liquid composition pointed towards an adsorption limited model. The model predicts a strong dependence of boron composition and a weak dependence of the phosphorous composition on the $[H_2PO_2^-]/[DMAB]$ ratio. That prediction was verified experimentally.

CoWBP thin films demonstrated high thermal stability and provided good barrier properties and can be applied as capping layers for ULSI copper metallization.

References

[1] C.K. Hu, J.M.E. Harper, Materials Chemistry and Physics 52 (1) (1998) 5–16.

[2] J. Gambino, T.L. McDevitt, F. Anderson, P. Felix, J. Gill, S.A. Mongeon, and J. Burnham, in: Proceedings of the Advanced Metallization Conference 2006 (AMC 2006), vol. 2006, pp. 501–507.

[3] A. Kohn, M. Eizenberg, Y. Shacham-Diamand, Applied Surface Science 212–213 (2003) 367–372.

[4] Y. Shacham-Diamand, Journal of Electronic Materials (2001) 336–344.

[5] Y. Shacham-Diamand, S. Lopatin, Electrochimica Acta (1999) 3639–3649.

[6] C.K. Hu, D. Canaperi, S.T. Chen, L.M. Gignac, B. Herbst, S. Kaldor, E. Liniger, D.L. Rath, D. Restaino, R. Rosenberg, J. Rubino, S.-C. Seo, A. Simon, S. Smith, W.-T. Tseng, in: Proceedings of the Reliability Physics Symposium Proceedings, 2004 pp. 222–228.

[7] A. Kohn, M. Eizenberg, Y. Shacham-Diamand, Applied Surface Science (2003) 367–372.

[8] A. Kohn, M. Eizenberg, Y. Shacham-Diamand, Journal Of Applied Physics (September) (2003) 3015–3024, p.1.

[9] N. Petrov, Y. Sverdlov, Y. Shacham-Diamand, Journal of the Electrochemical Society (2002) C187–C194.

[10] V. Bogush, Y. Sverdlov, H. Einati, Y. Shacham-Diamand, Proceedings of the Advanced Metallization Conference 2004 (AMC 2004), MRS publications, San Diego, USA, 2005, pp. 843–847.

[11] Y. Shacham-Diamand, Y. Sverdlov, V. Bogush, R. Ofek-Almog, Journal of Solid State Electrochemistry 11 (7) (2007) 929–938.